ORDER AND CHAOS IN MULTIDIMENSIONAL HAMILTONIAN SYSTEMS

Tassos BOUNTIS

Helen CHRISTODOULIDI and Christos EFTHIMIOPOULOS

Department of Mathematics and Center for Research and Applications of Nonlinear Systems (CRANS),

University of Patras, GR–26500, Rion, Patras, Greece

Energy Localization on Low–Dimensional Tori and the Interpretation of the FPU Paradox

INCT DE SISTEMAS COMPLEXOS Meeting, CBPF,

Rio de Janeiro, March 1–5, 2010

Contents

The Fermi-Pasta-Ulam (FPU) N-Degree-of-Freedom $\beta-$ Model

The FPU $\beta-$ model is a one–dimensional lattice of nonlinear oscillators described by the Hamiltonian

$$H = \frac{1}{2}\sum_{j=1}^{N} \dot{x}_j^2 + \sum_{j=0}^{N}\left(\frac{1}{2}(x_{j+1}-x_j)^2 + \frac{1}{4}\beta(x_{j+1}-x_j)^4\right) = E \tag{1}$$

E being its total energy. We want to understand its dynamics globally, as the value of $\beta > 0$ increases away from the linear case $\beta = 0$. We shall impose fixed boundary conditions:

$$x_0(t) = x_{N+1}(t) = 0, \ \forall t \tag{2}$$

We focus on **Simple Periodic Orbits**(SPOs), where all variables oscillate in or out of phase and return to their initial state after only one maximum and one minimum in their oscillation, i.e. **all characteristic frequencies are equal**. Examples of such SPOs are:

(a) **The SPO1 mode**, with N odd,

$$\hat{x}_{2j}(t) = 0,\ \hat{x}_{2j-1}(t) = -\hat{x}_{2j+1}(t) \equiv \hat{x}(t),\ j = 1, \ldots, \frac{N-1}{2}. \tag{3}$$

(b) **The SPO2 mode**, with $N = 5 + 3m,\ m = 0, 1, 2, \ldots$ particles,

$$x_{3j}(t) = 0,\ j = 1, 2, 3 \ldots, \frac{N-2}{3}, \tag{4}$$

$$x_j(t) = -x_{j+1}(t) = \hat{x}(t),\ j = 1, 4, 7, \ldots, N-1. \tag{5}$$

In the next slide, we show what these solutions look like for some small particle chains. These solutions are exact continuations of the $q = (N+1)/2$ and $q = 2(N+1)/3$ linear normal modes of the FPU chain described by the equations:

$$Q_q = \sqrt{\frac{2}{N+1}} \sum_{i=1}^{N} q_i \sin \frac{qi\pi}{N+1}, \qquad P_q = \dot{Q}_q \tag{6}$$

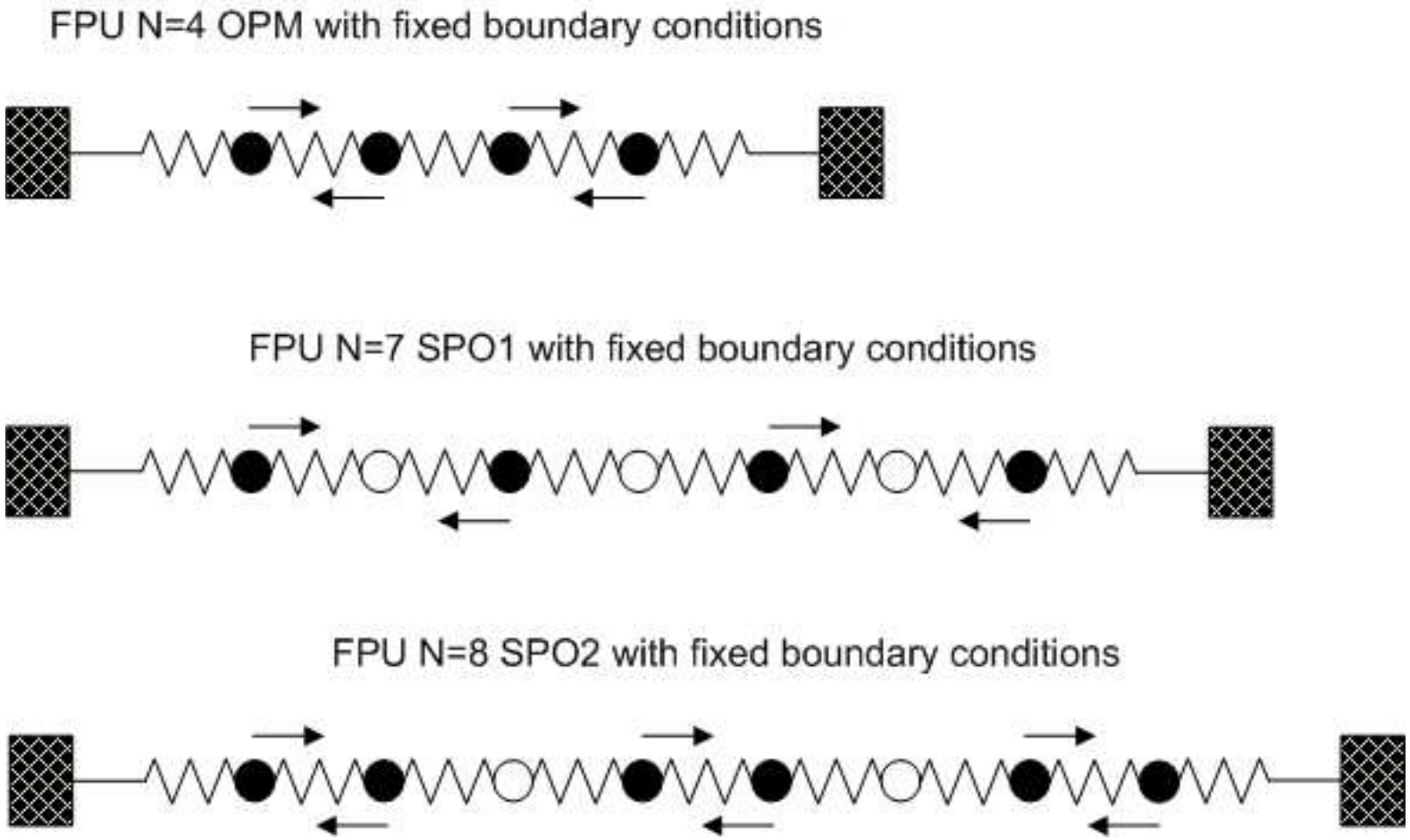

Figure 1: The SPO1 mode corresponding to every other particle being stationary and the SPO2 mode, with one stationary particle every other two.

with energies and frequencies

$$E_q = \frac{1}{2}\left[P_q^2 + {\Omega_q}^2 Q_q^2\right], \;\; \Omega_q = 2\sin\frac{q\pi}{2(N+1)} \tag{7}$$

What is of central importance here is to understand the paradox of the so–called **FPU recurrences**: As is well-known, Fermi, Pasta and Ulam (1956) observed numerically that, for $\beta > 0$ small, when the energy is placed initially in the $q = 1$ linear mode, very few other modes (7) become excited and all energy returns periodically to the q=1 mode. This is paradoxical, since it precludes the energy equipartition and ergodicity, expected by statistical mechanics generically from all nonlinear systems.

As a consequence of a theorem by Lyapunov, it is known that the linear modes of the FPU β – model can be continued as SPOs of the $\beta \neq 0$ nonlinear system. Viewing the **low** $q = 1, 2, 3, ..$ **modes** as SPOs and using linear stability analysis, Flach et al. (2005) report an approximate formula for their **destabilization energy**, given by

$$\frac{E_c}{N} \approx \frac{\pi^2}{6\beta N(N+1)} \tag{8}$$

Remarkably enough, this energy threshold for the destabilization of the low $q = 1, 2, 3..$ modes coincides with the "weak" chaos threshold shown by de Luca and Lichtenberg (1995) to lead to the **breakup of the FPU recurrences** through the interaction of low order resonances.
What is particularly interesting in the investigations of Flach et al. (2005) is their observation that FPU orbits obtained by exciting the above linear modes, when viewed **in Fourier q–space**, exhibit **exponential localization** reminiscent of discrete breathers in configuration space. Thus, they called these FPU solutions **q–breathers** and conjectured that their localization properties are somehow responsible for the FPU recurrences. They also suggested that their destabilization formula for the corresponding SPOs (8) is important due to its coincidence with the result by de Luca and Lichtenberg.

The main questions we wish to pose here are:
1) How exactly does the destabilization of these nonlinear modes and their q–localization properties affect the global properties of the motion?

2) How can we use the dynamics in the vicinity of these solutions to give a more complete interpretation of the paradox of the FPU recurrences?

Linear Stability of SPOs, Local and Global Chaos

Let us consider first our SPO1 and SPO2 orbits which have been chosen because their stability analysis can be performed exactly: For example, for the SPO1 mode, the equations of motion collapse to a single second order ODE:

$$\ddot{\hat{x}}(t) = -2\hat{x}(t) - 2\beta\hat{x}^3(t) \tag{9}$$

whose solution is well–known in terms of Jacobi elliptic functions with modulus κ^2,

$$\hat{x}(t) = \mathcal{C}\,\mathrm{cn}(\lambda t, \kappa^2) \tag{10}$$

Linearizing about this solution $x_j = \hat{x}_j + y_j$, by keeping up to linear terms in y_j, we get the variational equations

$$\ddot{y}_j = (1 + 3\beta\hat{x}^2)(y_{j-1} - 2y_j + y_{j+1}),\ j = 1, \ldots, N \tag{11}$$

These separate into N uncoupled Lamé equations

$$\ddot{z}_j(t) + 4(1 + 3\beta\hat{x}^2)\sin^2\left(\frac{\pi j}{2(N+1)}\right) z_j(t) = 0,\ j = 1, \ldots, N \tag{12}$$

where the z_j variations are simple linear combinations of the y_j's.

Changing variables to $u = \lambda t$, this equation takes the form

$$z_j''(u) + 2\big(1 + 4\kappa^2 - 6\kappa^2 \mathrm{sn}^2(u, \kappa^2)\big)\sin^2\left(\frac{\pi j}{2(N+1)}\right) z_j(u) = 0,\ j = 1, \ldots, N \qquad (13)$$

where primes denote differentiation with respect to u. According to Floquet theory, its solution is bounded (or unbounded) depending on whether the eigenvalues of the monodromy matrix are **on or off the unit circle**.

These periodic solutions all experience a first destabilization at energy densities:

$$\frac{E_c}{N} \propto N^{-\alpha},\ \alpha = 1,\ or,\ 2,\ N \to \infty. \qquad (14)$$

More specifically, the first variation $z_j(u)$ to become unbounded as κ^2 (or, the energy E) increases is $j = \frac{N-1}{2}$ and the energy values $E_c/N \propto 1/N$ at which this happens are plotted below.

We have discovered that the energy threshold for the low q orbits, (8), **coincides** with the instability threshold of our SPO2 mode. Below we compare formula (22) (dashed line) with the destabilization threshold for our SPO2 and find excellent agreement.

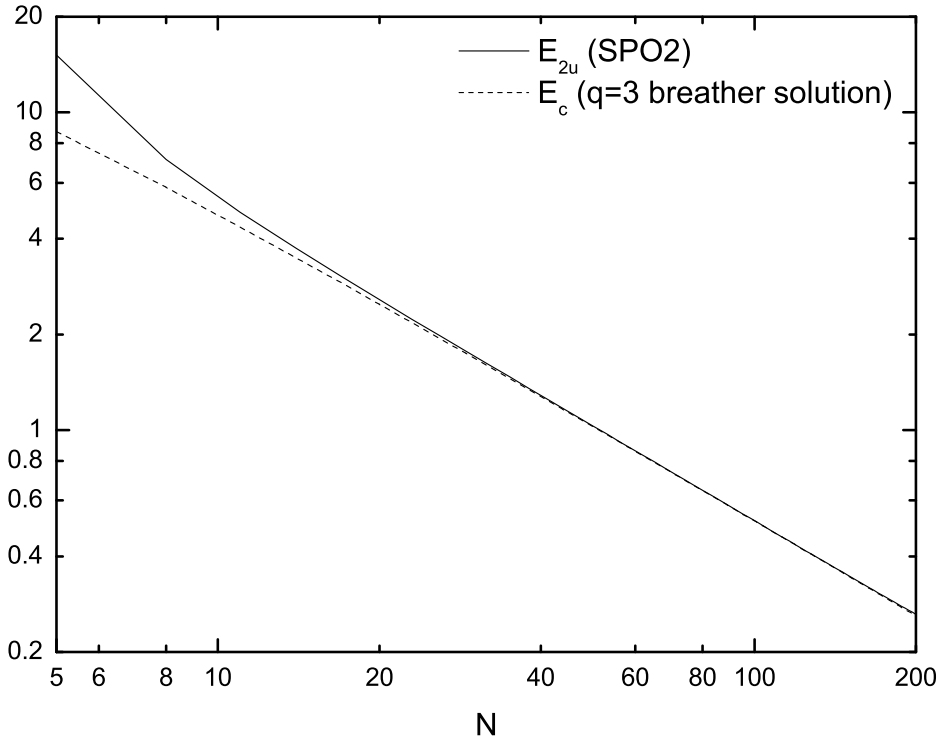

Figure 2: The solid curve is the energy E_c/N of the first destabilization of the SPO2 (**the** $q = 2(N+1)/3$ **mode**) for $\beta = 0.0315$ obtained from the eigenvalues of the monodromy matrix and the dashed line is the approximate formula (22)$\sim 1/N^2$.

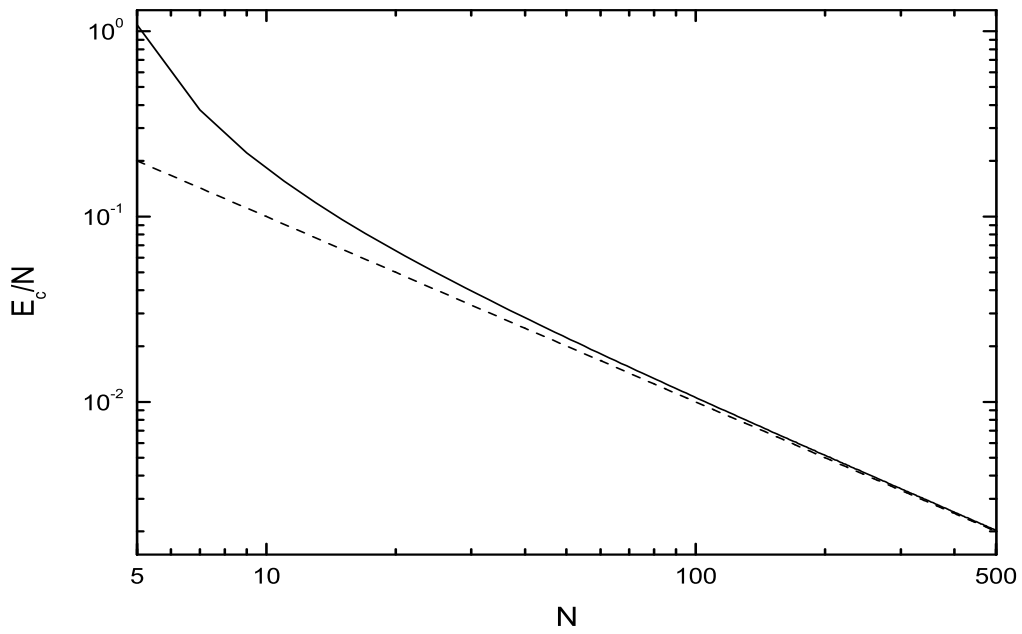

Figure 3: Concerning the SPO1 solution of the FPU system, we plot here the energy $\frac{E_c}{N}$ of the first destabilization of the (**the** $q = (N+1)/2$ **mode**) obtained by the monodromy eigenvalues. The dashed line is the function $\propto \frac{1}{N}$. As we shall see in the next figure this SPO is related to the presence of global chaos in the system.

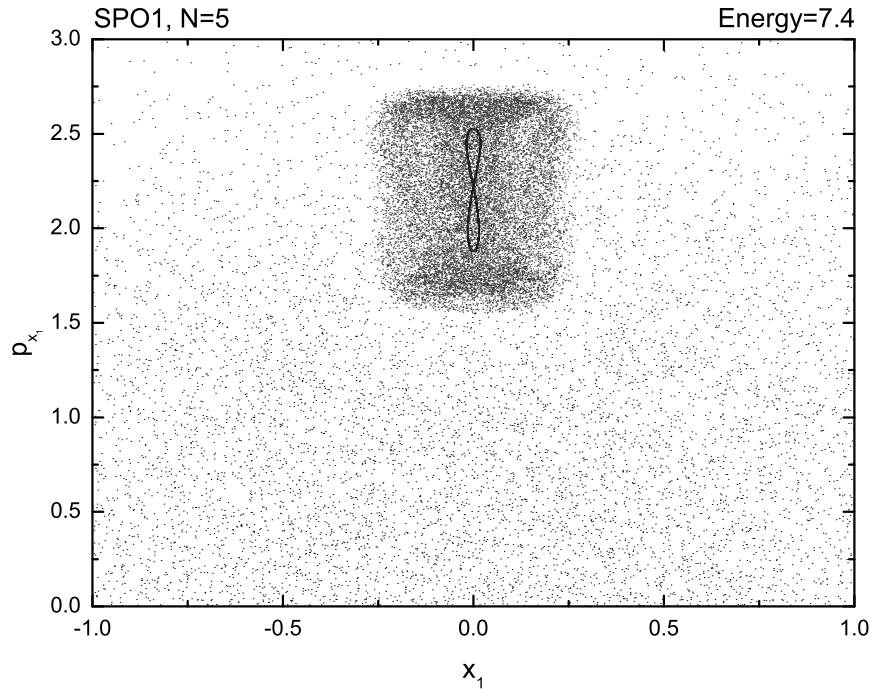

Figure: Global chaos is connected with the destabilization of the SPO1 orbit. Note the nested chaotic regions for initial conditions in the immediate vicinity ($\simeq 10^{-5}$) of the unstable SPO1 orbit, then at ($\simeq 10^{-2}$), where we see a vague resemblance to "figure eight" and a large scale chaotic region for more distant initial conditions ($\simeq 0.1$) for $N = 5$ particles, on the Poincaré surface of section $(x_1, \dot{x}_1)$ taken when $x_3 = 0$. In this picture we integrated our orbits up to $t_n = 10^5$ in the energy surface $E = 7.4$.

q–Breathers, q–Tori and the FPU Paradox

Following, for $\beta > 0$ small, one of the first q–modes, say $q = 1$, as an **exact SPO** of the FPU lattice, we find that its main harmonic excites (through nonlinearity), very few other harmonics, whose amplitudes are **exponentially localized** in Fourier (q–) space.

This was called by Flach et. al (2005) a **q-breather** and offers new insight in the understanding of the problem of energy localization and the **long term deviations from equipartition** among the modes, i.e. the origin of the famous **paradox of the FPU recurrences**.

The first important property of the q-breathers is that **their energy profiles** $E(q)$ are **very similar** with the profiles of the numerically computed 'FPU-trajectories' (where the energy is initially placed in one of the linear modes). Furthermore, it is intriguing that this localization persists even for values of the parameters (coupling, energy and N) for which the corresponding **q-breather periodic solution has become linearly unstable!**.

How can we understand these dynamical phenomena in relation to the FPU paradox?

Previous work by de Luca et al. (1998) and Berchialla et al. (2004, 2005) has shown that FPU–recurrences also arise if a (low-frequency) **part of the spectrum** is initially excited. Thus, long before equipartition, one observes the formation of **metastable states coined 'natural packets'**, exhibiting a kind of internal equipartition among the participating modes.

In our work, we aim to **reconcile these two approaches**, i.e.: (a) The interpretation based on the q-breathers and (b) the analysis based on the above metastable states.

Nekhoroshev stability estimates also show that **all the FPU-trajectories starting close to a stable q-breather solution are exponentially stable**. This leads to the idea that the FPU-trajectories could be understood in terms of classes of solutions lying on **tori of low dimension** $2 \leq s << N$, being the continuations of the motions resulting from exciting s modes of the uncoupled case.

Thus, generalizing the concept of q-breathers, we call **'q-tori'** the solutions on such low-dimensional tori and demonstrate i) their existence, and ii) the validity of energy localization laws analogous to those found for the q-breathers.

Our analytical theory of the q-tori uses of **the Poincaré - Lindstedt method** and yields scaling laws for the energy profile $E(q)$ of a trajectory lying on a q-torus. Numerically, we also find that for **FPU trajectories** (which start on the linear normal modes) **energy localization persists for long times** even when there are indications that the **q-torus is unstable**.

As a numerical criterion for the **stability of q-tori** we use the recently developed **method of 'Generalized Alignment Indices'** (GALI, Skokos et al. 2006). Through the GALI method, we find that low-dimensional tori destabilize at approximately the same parameter values where the q-breathers turn unstable.

We have obtained analytical results on the **existence and scaling laws** of the 'q-tori', starting with the proof of a proposition which establishes which set of modes are excited **recursively** at the $k-$th order of the Poincare Linstedt theory. We then focus on the 'q-tori', corresponding to lowest order excitations of a set of adjacent modes $q_{0,i} = i$, $i = 1, \ldots, s$, whose energy profile $E(q)$ is calculated analytically and tested against numerical integration (see Figs. 1 and 2 below).

Let us use an example with $N = 8$ particles, whose solutions lie on a **two-dimensional torus** representing the continuation, for $\beta \neq 0$, of the quasi-periodic solution of the uncoupled ($\beta = 0$) system $Q_1(t) = A_1 \cos \Omega_1 t$, $Q_2 = A_2 \cos \Omega_2 t$, for a suitable choice of A_1 and A_2.

Following the Poincaré - Lindstedt method we look for solutions $Q_q(t)$, $q = 1, \ldots, 8$ expanded as series in the parameter $\sigma = \beta/2(N+1)$, namely

$$Q_q(t) = Q_q^{(0)}(t) + \sigma Q_q^{(1)}(t) + \sigma^2 Q_q^{(2)}(t) + \ldots, \; q = 1, \ldots 8 \; . \tag{15}$$

For the motion to be quasi-periodic on a **two–torus** and represent a continuation of the unperturbed solutions Q_1 and Q_2, the functions $Q_q^{(r)}(t)$ must, at any order r, be trigonometric polynomials involving only two frequencies, ω_1 and ω_2, which are small corrections of the normal mode frequencies Ω_1, Ω_2 and are given as series in powers of σ, namely:

$$\omega_q = \Omega_q + \sigma \omega_q^{(1)} + \sigma^2 \omega_q^{(2)} + \ldots, \; q = 1, 2 \; . \tag{16}$$

so that secular terms (of the form $t \sin \omega_q t$ etc.) in the solutions $Q_q(t)$ are eliminated.

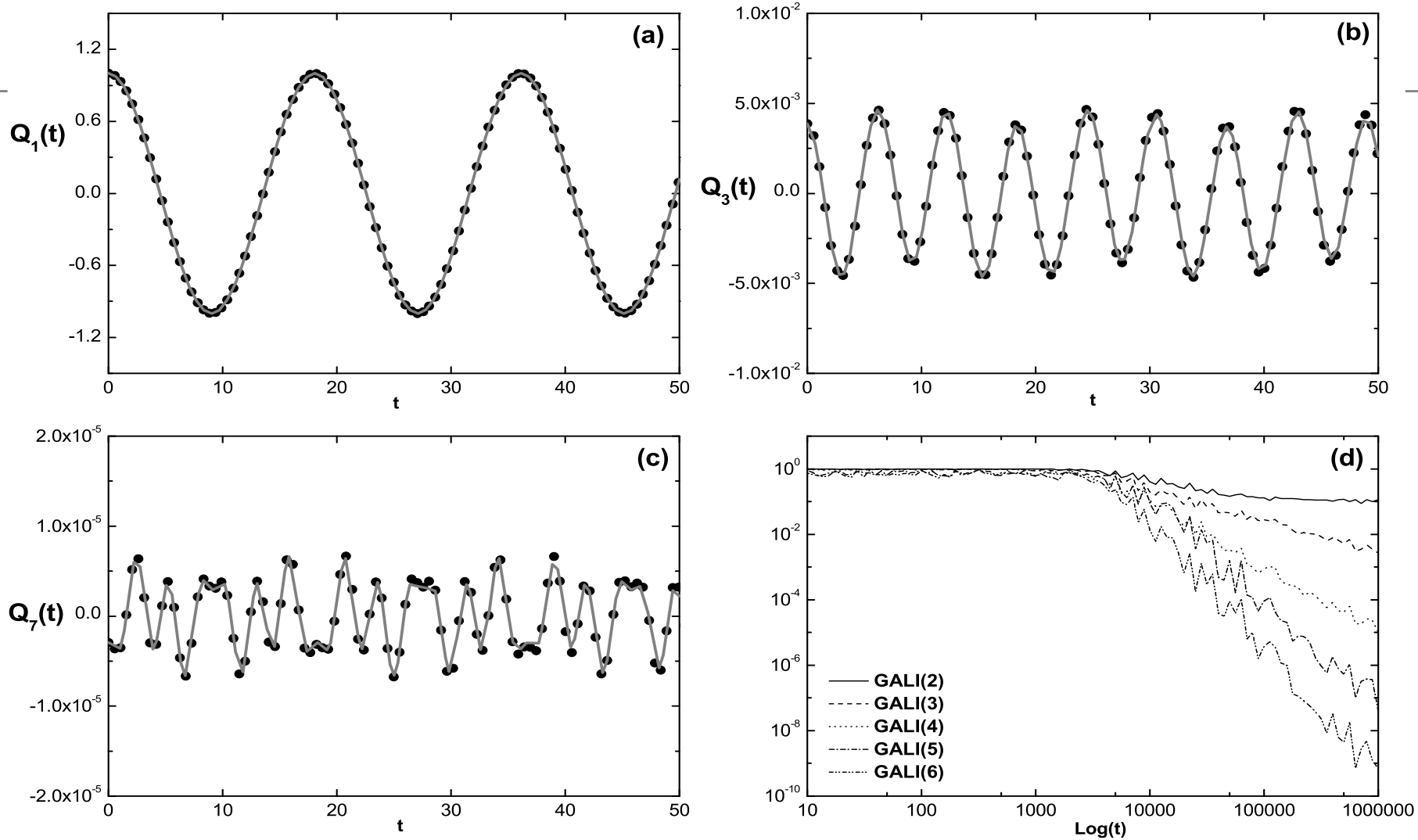

Figure 4: Comparison of numerical (points) versus analytical (solid line) solutions, using the Poincaré - Lindstedt series up to order $O(\sigma^2)$, for the temporal evolution of the modes (a) $q = 1$, (b) $q = 3$, and (c) $q = 7$, when $A_1 = 1$, $A_2 = 0.5$, and $N = 8$, $\beta = 0.1$. The temporal evolution of the indices $GALI_2$ to $GALI_6$, up to a time $t = 10^6$ is shown in (d).

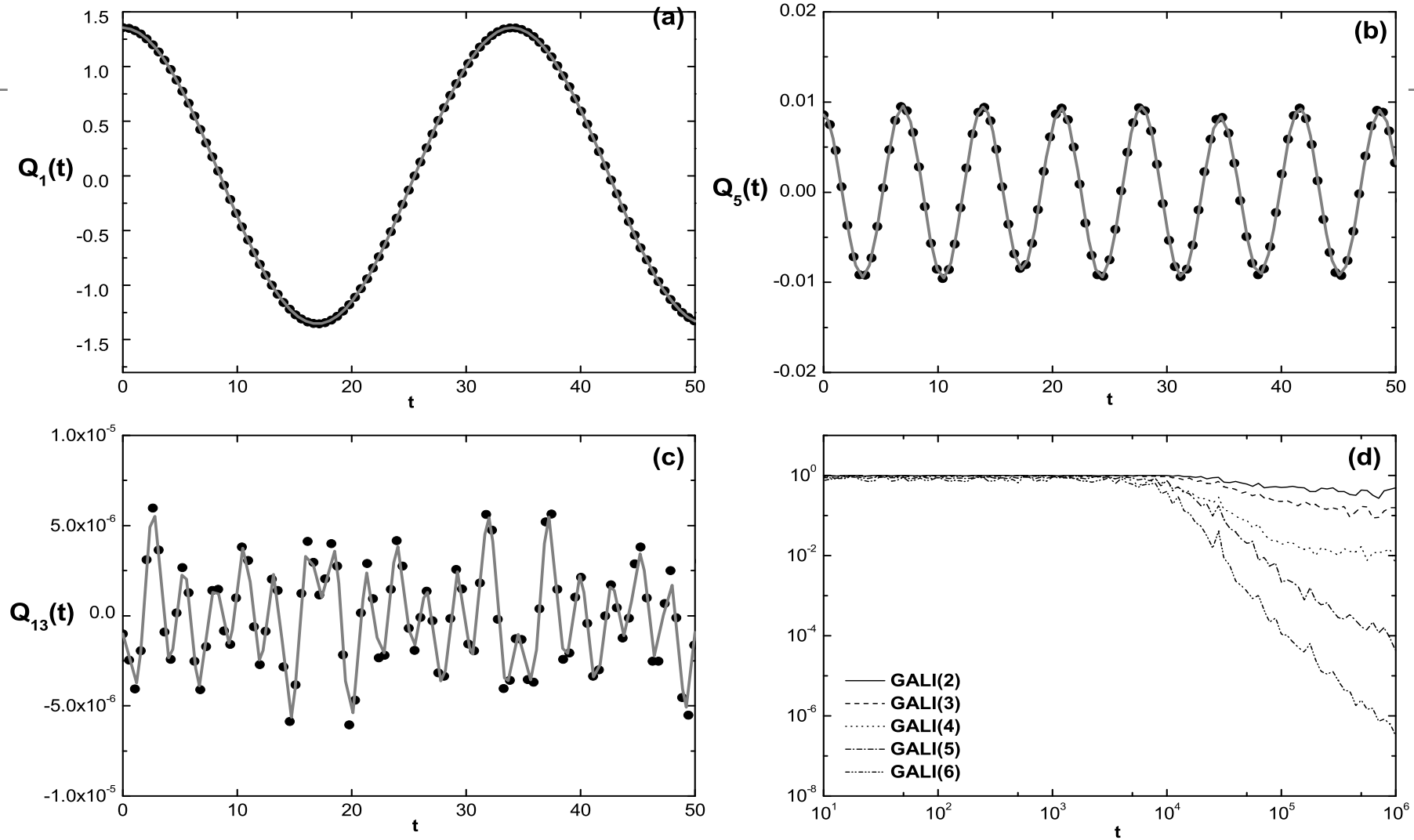

Figure 5: This shows the existence of a 4-torus with $N = 16$, $\beta = 0.1$, when 4 modes are initially excited. The temporal evolution $Q_q(t)$ is shown for the modes (a)$q = 1$, (b)$q = 5$, (c)$q = 13$. The $GALI_k$, $k = 2, 3, 4$ indices, are seen to stabilize at $t \geq 10^5$, while for $k \geq 5$ the indices continue to decrease by power laws.

Scaling Laws of the Harmonic Energies

Figure 6 shows the average harmonic energy of each of the modes over a time span $T = 10^6$ for the case of the q-torus of Figure 4, shown in Fig. 6a, and the torus of Fig. 5 shown in Fig. 6b respectively. The numerical result compares excellently with the analytical result obtained via the Poincaré - Lindstedt method. The line of red circles shows a 'stepwise' estimate of the localization profile in **groups of modes** excited at the consecutive orders of the recursive scheme, as will be explained below.

The average harmonic energies of all modes of the group $k = 1$ are given by

$$E_q^{(1)} = \frac{12^2 \omega_1^2 (q^{(1)})^2 A_0^6}{((q^{(1)})^3 - \mid \pm q_{i_1}^3 \pm q_{i_2}^3 \pm q_{i_3}^3 \mid)^2} \ . \tag{17}$$

A theoretical estimate of this type is shown by the blue triangles in Fig. 6, for the orbits lying on q-tori. Namely, in Fig. 6a we see clearly that the decrease of the **average energy takes place by abrupt steps**, with three groups formed at nearby energies, namely the groups of modes 1,2, then 3 to 6, and then 7,8, i.e., as expected by the recursive scheme and reproduced very well by the numerical calculations (empty circles). The phenomenon is also seen in Fig. 6b, where the grouping of the modes is (1 to 4), (5 to 12), (13 to 16).

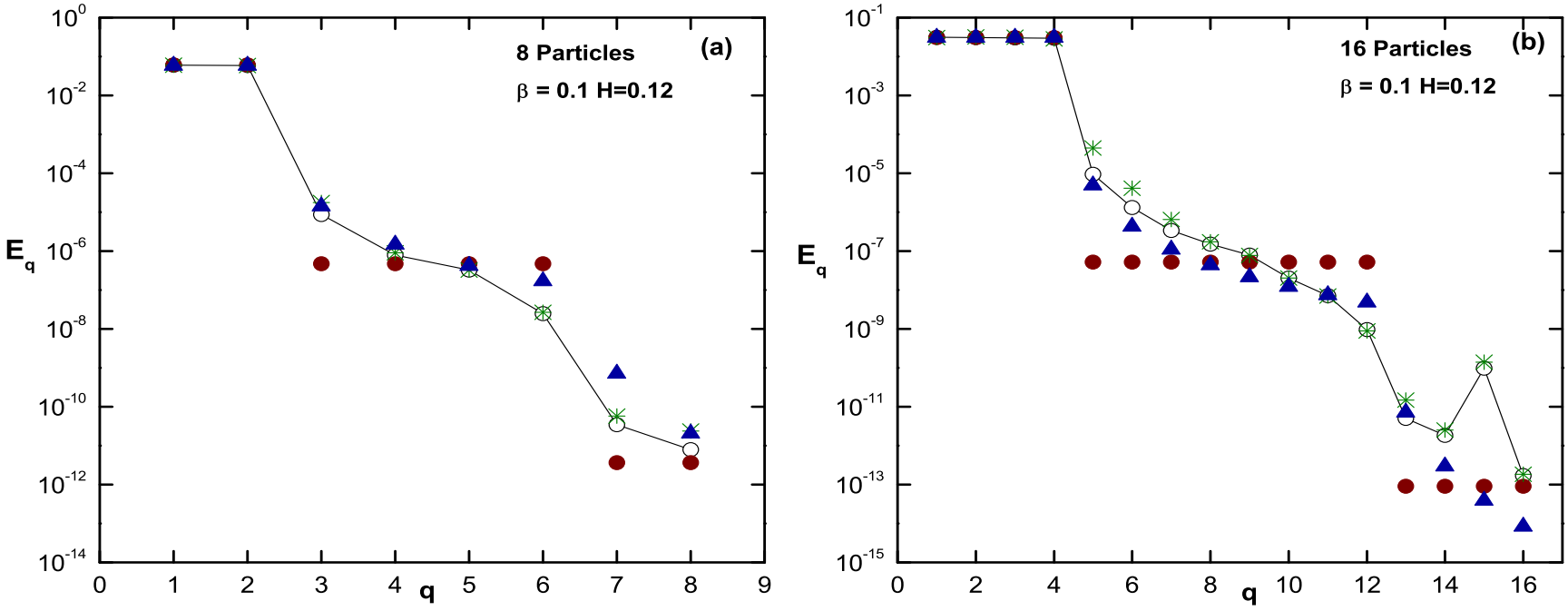

Figure 6: The average harmonic energy E_q of the q-th mode as a function of q, after 10^6 periods for (a) the 2-torus and (b) 4-torus solutions corresponding to the initial conditions as in Figs. 4 and 5, shown numerically by empty circles. The stars indicate E_q via the analytical solutions $Q_q(t)$ of the Poincaré -Lindstedt series, see Eq.(17). The blue triangles are based on theoretical estimates of the amplitudes of the leading terms of the series. The red circles show a theoretical estimate based on the average energy of each group, see Eq.(20) below.

A Theoretical Estimate of the Energy Profile

Let us obtain an estimate for the average harmonic energies $E^{(k)}$ of the modes $q^{(k)} = (2k+1)s - O(s/N)$ excited at the kth order of the perturbation theory. The total energy E is estimated as the sum of all the energies of the modes $1, \ldots, s$ and gives

$$E \sim s\omega^2_{q^{(0)}} A_0^2 \sim \frac{\pi^2 s^3 A_0^2}{N+1} \ .$$

On the other hand, the energy of each of the modes $q^{(k)}$ can be estimated as

$$E^{(k)} \sim \frac{1}{2}\omega^2_{q^{(k)}} \left(\frac{\beta}{2(N+1)}\right)^{2k} (A^{(k)})^2 \sim \frac{\pi^2 s^2 (Cs\beta)^{2k} A_0^{4k+2}}{2^{2k+1}(N+1)^{2k+2}}$$

which, in terms of the total energy E, yields

$$E^{(k)} \sim \frac{E}{s}\left(\frac{C^2\beta^2(N+1)^2E^2}{\pi^4 s^4}\right)^k \ . \qquad (18)$$

The similarity of Eq.(18) with the corresponding equation for q-breathers is obvious, where according to (Flach et al. 2006)

$$E_{(2k+1)q_0} \sim E_{q_0} \left(\frac{9\beta^2 (N+1)^2 E^2}{64\pi^4 q_0^4} \right)^k \tag{19}$$

where q_0 is the unique mode excited at the zeroth order of the perturbation theory. Note that the integer s plays in Eq.(18) a role similar to that of q_0 in Eq.(19). This means that the energy profile of a q-breather with $q_0 = s$ presents the same exponential law as the energy profile of the s-torus solution.

Another important feature of these solutions is that the **profile remains unaltered** as N increases provided that i) **a constant fraction** $M = s/N$ of the spectrum is initially excited, i.e. that s increases proportionally to N, and ii) the **specific energy** $\epsilon = E/N$ **remains constant**. Indeed, in terms of the specific energy ϵ, (18) becomes **independent of** N

$$E^{(k)} \sim \frac{\epsilon}{M} \left(\frac{C^2 \beta^2 \epsilon^2}{\pi^4 M^4} \right)^k \tag{20}$$

In Fig.6, we saw that the theoretical estimate (18) fits nicely the exact profiles for the q-tori solutions obtained numerically. The key question, now, is:

Does Eq.(18) retain its predictive power in the case of generic FPU trajectories which, by definition, start close to, but not exactly on a q-torus solution?.

The answer is partly contained in the results of Figures 7 and 8 below: Figure 7 shows the energy localization profile in numerical experiments in which β is kept fixed, and N takes the values $N = 16$, $N = 32$ and $N = 64$.

In all 3 cases the FPU-trajectories are calculated numerically, starting with initial conditions in which *only* $s = 2$ (for $N = 16$), $s = 4$ (for $N = 32$) and $s = 8$ (for $N = 64$) modes are excited at $t = 0$. These trajectories differ from q-tori solutions in that in the q-tori solutions all the modes have some excitation initially, while in the case of the FPU trajectories only the s first modes are excited at $t = 0$.

This is exemplified in Figs.7a,b,c, in which the average energy profiles of the FPU-trajectories after the time $t = 10^6$ exhibit the same **'stepwise' behavior** as predicted by Eq.(18), for an exact s-torus solution with the same total energy as the examined FPU trajectory.

In particular, the modes of Fig.7a are clearly separated in groups, (1 to 4), (5 to 12) and (13 to 20),etc., as foreseen for an exact 4-torus solution. The energies of all the modes in one group exhibit a kind of 'plateau' at nearly the values predicted by Eq.(18). Similar plateaus are distinguishable also in Figs.7b,c for an FPU solution close to an 8-torus and a 16-torus respectively.

Now, the lower row of Fig.7 shows what happens when the specific energy of FPU-trajectories **is increased by a factor 10** with respect to the panels in the top row: The sharp plateaus are gradually lost in the profiles of the FPU-trajectories. Despite that, however, the energy profiles **retain their exponential decay** with increasing mode number q, and, more importantly, the slope of the exponential decay law continues to be essentially predicted by Eq.(18). This indicates that the FPU trajectories of Figs.7d,e,f are still relatively close to q-tori solutions with the same total energy.

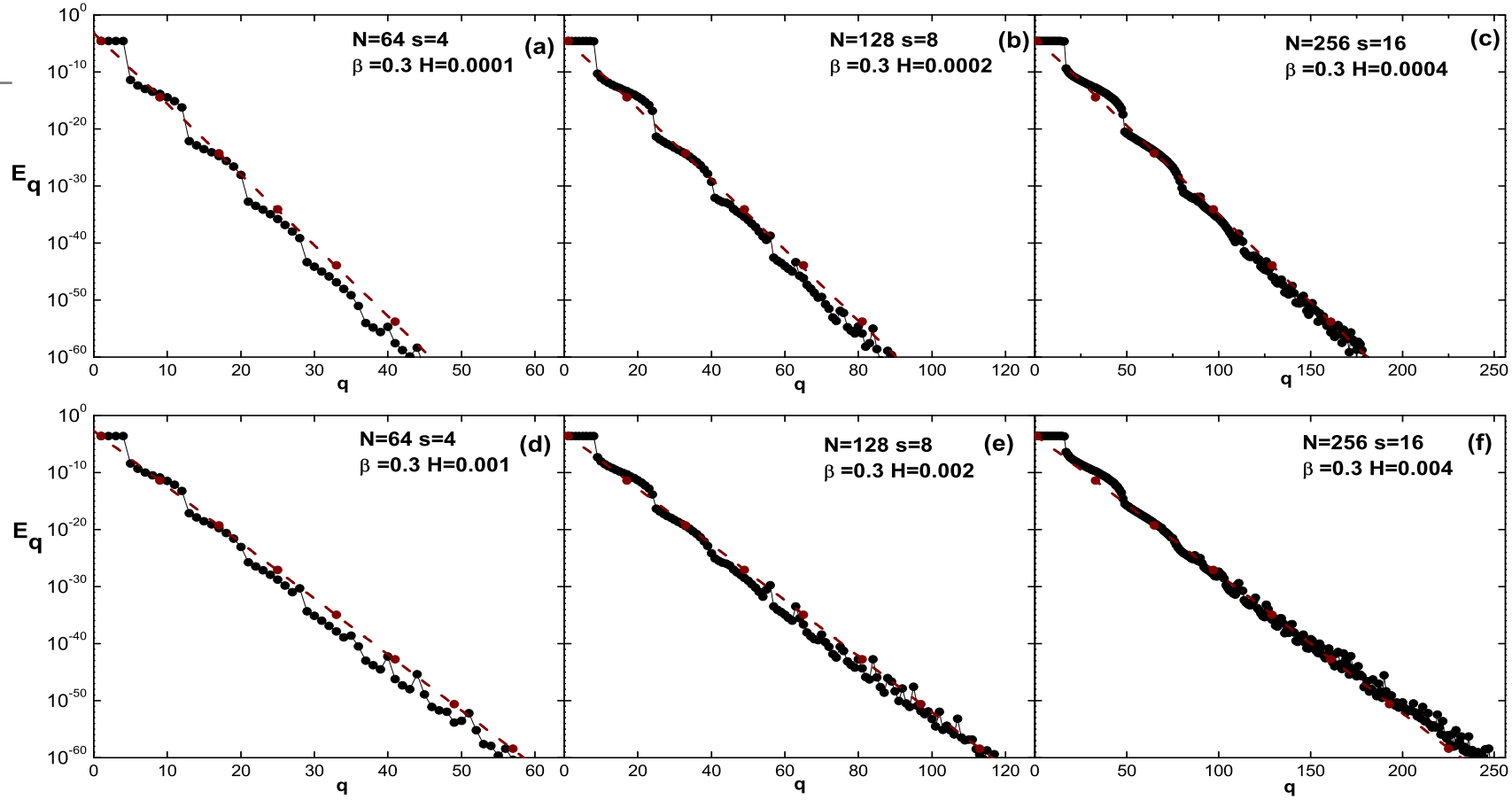

Figure 7: The average harmonic energy E_q of the q-th mode as a function of q in various examples of FPU-trajectories, for $\beta = 0.3$, in which the $s(= N/16)$ first modes are excited initially so that the total energy is $E = H$ as indicated in each panel. The specific energy is constant, i.e. $\varepsilon = 1.5625 \times 10^{-6}$ in the top and $\varepsilon = 1.5625 \times 10^{-5}$ in the bottom row. The dashed lines represent the average exponential profile E_q obtained by the assumption that the FPU trajectories lie close to q-tori governed by (20).

When we increase the energy further, the FPU-trajectories deviate from the s-tori solutions and the energy profiles of the FPU-trajectories also deviate from the energy profiles of the s-tori. The profiles of the FPU-trajectories are smoother and the groups of modes less distinct, while retaining the average exponential slope as predicted by Eq.(20). This is evident in Fig. 8a, in which the energy is increased by a factor 50 with respect to Fig. 7d, for the same N and β. Also, in Fig. 8a we observe an overall rise of the localization profile at the high-frequency part of the spectrum. This is shows that the system tends towards **equipartition**.

The important point is that **exponential localization** of the FPU trajectories persists and is still characterized by Eq.(18). Furthermore, at energies beyond a threshold value, an interesting phenomenon occurs: For fixed N (see e.g. Figure 8, where $N = 64$), as the energy increases, a higher value of s needs to be used in Eq.(18), so that the theoretical profile yields an exponential slope that agrees with the numerical data. When $\beta = 0.3$, $N = 64$, this value is $E \approx 0.1$ and splits the system in two distinct regimes: One for $E < 0.1$, where the numerical data are well fitted by a choice of $s = 4$ in Eq.(18) and another for $E > 0.1$, where Eq.(18) suggests that s increases with the energy, e.g. $s = 6$ for $E = 0.2$, rising to $s = 12$ for $E = 0.5$.

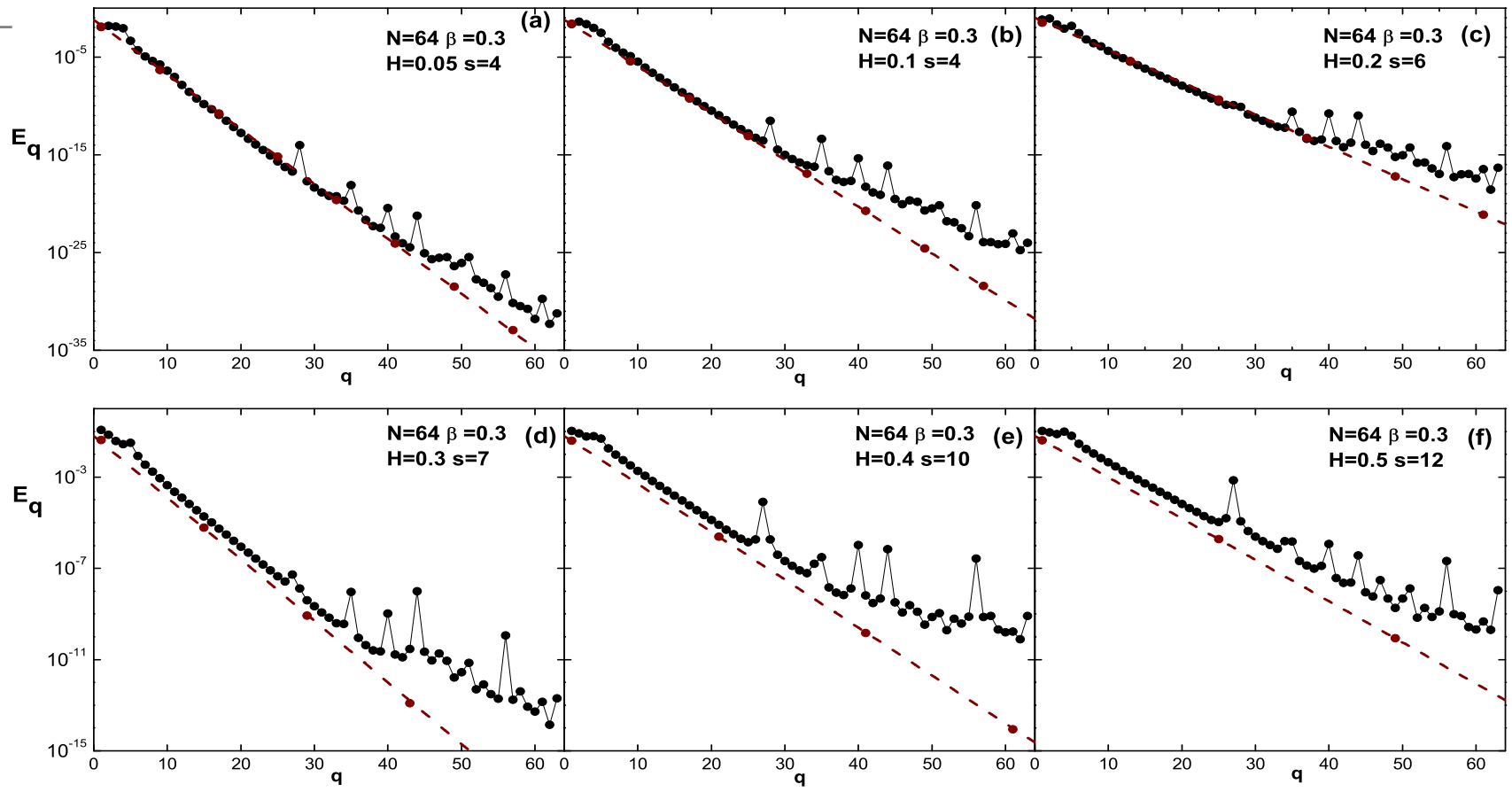

Figure 8: Same as in Fig. 7a but for larger energies, namely (a) $E = 0.05$, (b) $E = 0.1$, (c) $E = 0.2$, (d) $E = 0.3$, (e) $E = 0.4$, (f) $E = 0.5$. Beyond the threshold $E \simeq 0.1$, theoretical profiles of the form (18) yield the correct exponential slope if s is gradually increased from $s = 4$ in (a) and (b) to $s = 6$ in (c), $s = 7$ in (d), $s = 10$ in (e), and $s = 12$ in (f).

This indicates that the FPU-trajectories are closer to s-tori with a **higher** value of s ($s > 4$), despite the fact that only the 4 first modes are initially excited.

These results are in agrement with the 'natural packet' scenario described in Berchialla et al. (2004), who established numerically the formation of **metastable states**, in which a packet of modes is seen to share the total energy. An analogous behavior is suggested by Fig. 8, where the width of the packet increases beyond $M = 1/16$ (corresponding to $s = 4$ for $N = 64$), only above a certain energy threshold. Above this threshold it tends to stabilize as E increases, as seen Fig. 8d,e,f. According to Eq.(18), this implies that in the second regime the width s depends asymptotically on E as $s \propto E^{1/2}$, or, from Eq.(20) $M \propto \varepsilon^{1/2}$. This agrees well with estimates on the width of natural packets formed by the $\beta-$FPU model as described in Lichtenberg et al. (2008).

Stability of the motion near q-tori

The linear **stability of q-breathers can be studied by Floquet theory**, which demonstrates that a q-breather is linearly stable as long as

$$R = \frac{6\beta E_{q_0}(N+1)}{\pi^2} < 1 - O(1/N^2) \tag{21}$$

This is obtained by analyzing the eigenvalues of the monodromy matrix of the linearized equations about a q-breather solution constructed by the Poincaré - Lindstedt series. In the case of q-tori, however, this analysis does not apply. Nevertheless, an approximate numerical criterion for **the stability of q-tori is provided by the GALI indices**, see Skokos et al. (2007). According to this method, if a q-torus becomes unstable beyond a critical parameter, the deviation vectors of trajectories lying on the torus fall exponentially fast on the unstable manifold of the q-torus.

In practice, the exact dimension of the torus is unknown. However, if one starts in its vicinity, the trajectories are weakly chaotic and hence **all GALI indices start to fall exponentially**, after a transient time. Thus, to check torus instability, it suffices to calculate the time evolution of the lowest index, $GALI_2$.

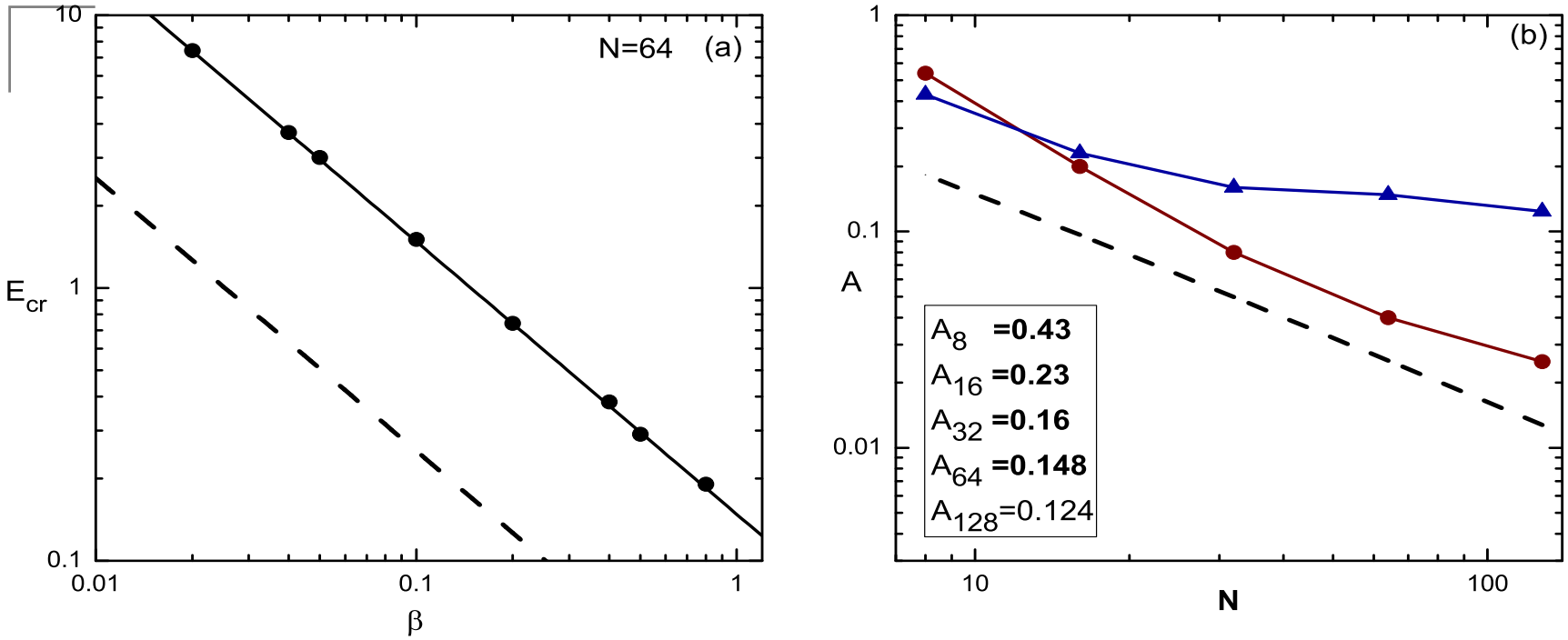

Figure 9: (a) The energy E_c at which the $GALI_2$ index of a FPU-trajectory started by exciting the modes $q = 1$, $q = 2$ loses its constancy, as a function of β, for $N = 64$. The solid line is a power-law yielding $E_c = A\beta^{-1}$, with $A = 0.148$ for $N = 64$. (b) The upper curve shows the dependence of the fitting constant A on N when the critical energy E_c is determined as in (a), for different values of N. The lower and middle curves correspond to a similar calculation of A vs. N for q-breather solutions ($q_0 = 1$) and for FPU trajectories started by exciting initially only the $q = 1$ mode. In both cases A varies with N as N^{-1}. The dashed lines in both panels represent the law of Eq.(21).

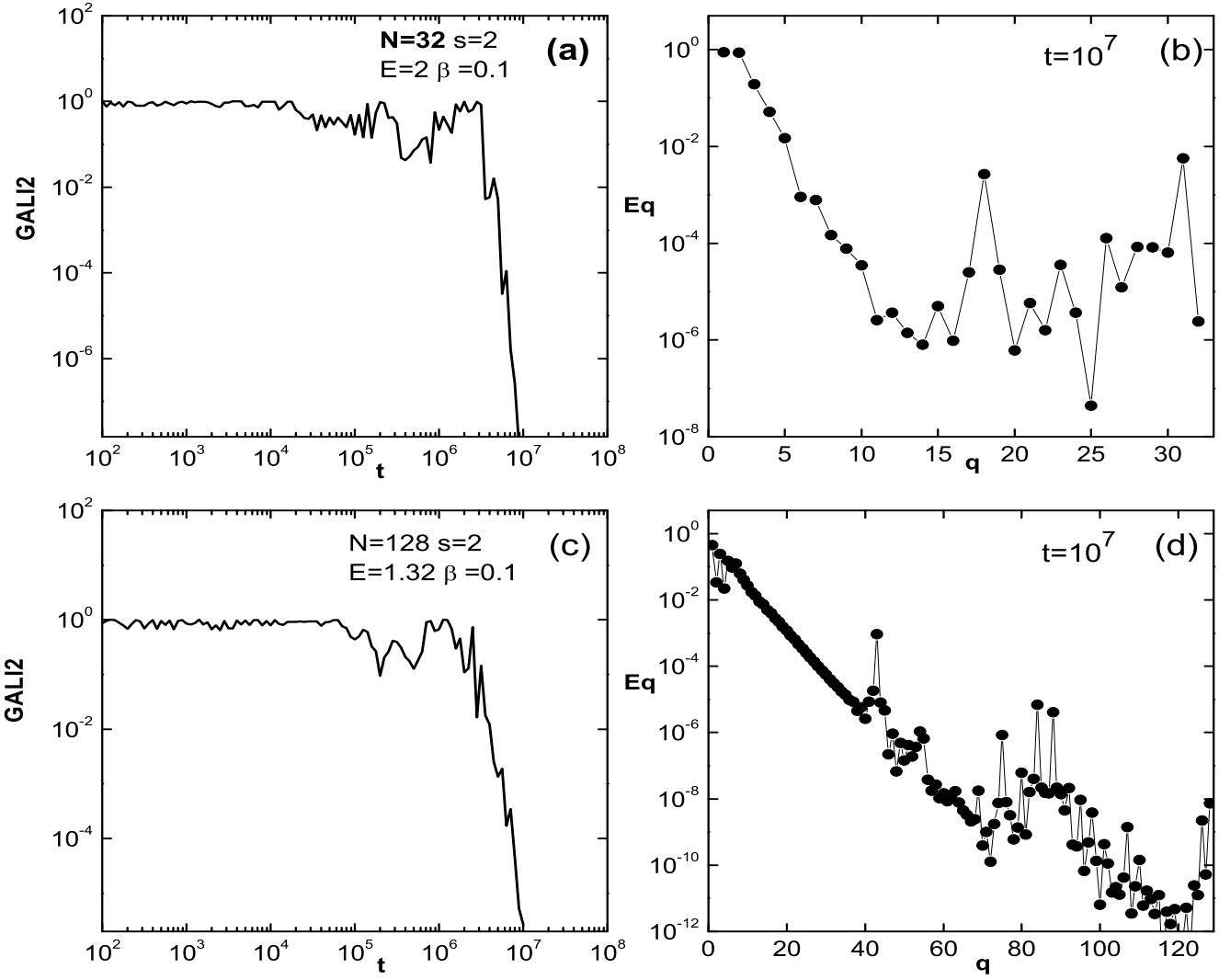

Figure 10:(a) Time evolution of the $GALI_2$ index up to $t = 10^7$ for an FPU trajectory started by the $q = 1$ and $q = 2$ modes for $N = 32$, $\beta = 0.1$, with total energy $E = 2 > E_c = 1.6$. (b) Energy localization profile of the FPU trajectory of (a) at $t = 10^7$. (c) Same as in (a) for $N = 64$, $E = 1.323$. (d) Same as in (b) for the trajectory of (c).

The most important remark concerning the linear stability of q-breathers or q-tori is that the exponential localization of FPU trajectories persists even after the associated q-breathers or q-tori have been identified as linearly unstable by the GALI criterion. This behavior is exemplified in Figure 10, where panels (a) and (c) show the time evolution of the $GALI_2$ index for two FPU trajectories started in the vicinity of 2-tori of the $N = 32$ and $N = 128$ systems, when $\beta = 0.1$ and $t_{max} = 10^7$.

In both cases the energy satisfies $E > E_c$, thus the exponential fall-off of the $GALI_2$ index is already observed at $t = 10^7$. However, a simple visual inspection of Figs. 10b,d clearly shows that the exponential localization of the energy persists in the Fourier space of both systems. In fact, we have found that exponential localization is found to persist for energies much larger than E_c, but for timescales which become smaller as E increases.

Nekhoroshev Stability

Clearly, **linear stability does not suffice** to explain the persistence of exponential localization of the FPU trajectories for very long times. Thus, we now investigate the long term stability of FPU trajectories in the spirit of the **Nekhoroshev** theory. In particular, we implement a scheme proposed by Giorgilli (1988), which employs the approximate integrals of the system determined as polynomial series in the canonical variables. In the case of simple polynomial Hamiltonians like $H = H_2 + H_4$ this algorithm simplifies considerably the calculations concerning the asymptotic properties of the series.

Approximate integrals of motion

If we define the complex conjugate canonical variables (q_j, p_j) via the inverse of the linear canonical transformation

$$Q_j = \frac{q_j + ip_j}{\sqrt{2\Omega_j}}, \; P_j = \frac{iq_j + p_j}{\sqrt{2/\Omega_j}} \; , \tag{22}$$

the Hamiltonian of the $\beta-$ FPU chain takes the following form

$$H = H_2 + H_4 = \sum_{j=1}^{N} i\Omega_j p_j q_j + \frac{\beta}{8(N+1)}$$

$$\times \sum_{q,l,m,n=1}^{N} C_{q,l,m,n} (\Omega_q \Omega_l \Omega_m \Omega_n)^{1/2} (q_q + ip_q)(q_l + ip_l)(q_m + ip_m)(q_n + ip_n) \quad (23)$$

If $\beta = 0$, all $E_j = i\Omega_j p_j q_j$ are exact integrals of motion. We thus construct approximate integrals of motion for to the $\beta \neq 0$ case, using the series

$$\Phi_j = \Phi_j^{(2)} + \Phi_j^{(4)} + ... \quad (24)$$

where $\Phi_j^{(r)}$ is an rth degree polynomial in the variables $(q_1, \ldots, q_N, p_1, \ldots, p_N)$, and $\Phi_j^{(2)} \equiv E_j = i\Omega_j p_j q_j$. Since the series (24) represents an integral of the motion its Poisson bracket with the Hamiltonian should vanish.

This condition can be **satisfied formally**, if an appropriate choice is made for the terms $\Phi_j^{(r)}$, since the Poisson bracket condition $\{\Phi_j^{(2)} + \Phi_j^{(4)} + ..., H_2 + H_4\} = 0$ splits into an infinite number of equations of the form

$$\{\Phi_j^{(r-2)}, H_4\} + \{\Phi_j^{(r)}, H_2\} = 0,\ r = 4, 6, ... \tag{25}$$

Eq.(25) can be solved for the unknown function $\Phi_j^{(r)}$ provided that the function $\Phi_j^{(r-2)}$ is known from the previous step. This scheme is complete since we have set $\Phi_j^{(2)} = i\Omega_j p_j q_j$, equal to the harmonic energy of the j-th mode. The solution of (25) is particularly simple in the canonical variables (q, p).

Given the definition of H_2 and H_4 via the two sums on the r.h.s. of (23), and using the compact notations

$$\mathbf{q^m p^n} \equiv q_1^{m_1} q_2^{m_2} \ldots q_N^{m_N} p_1^{n_1} p_2^{n_2} \ldots p_N^{m_N}$$

$$\mathbf{m} \equiv (m_1, m_2, \ldots, m_N),\ m \equiv m_1 + m_2 + \ldots + m_N$$

(similarly for $\mathbf{n}$), the Poisson bracket $\{\Phi_j^{(r-2)}, H_4\}$, takes the form of a polynomial of r-th degree:

$$\{\Phi_j^{(r-2)}, H_4\} = \sum_{m,n=1, m+n=r}^{r} h_{m,n}^{(r)} \mathbf{q^m p^n}\ . \tag{26}$$

Using the above definition of H_2, the solution of (25) for the unknown function $\Phi_k^{(r)}$ is readily obtained as:

$$\Phi_j^{(r)} = - \sum_{m,n=1, m+n=r} \frac{h_{m,n}^{(r)} \mathbf{q}^{\mathbf{m}} \mathbf{p}^{\mathbf{n}}}{(\mathbf{m}-\mathbf{n}) \cdot \mathbf{\Omega}} \ . \tag{27}$$

To proceed, the frequencies $\mathbf{\Omega} \equiv (\Omega_1, \Omega_2, \ldots \Omega_N)$, given by Eq.(7) must be completely non-resonant, i.e., no integer vector $\mathbf{M} \neq (0, 0, \ldots, 0)$ exists such that $\mathbf{M} \cdot \mathbf{\Omega} = 0$ (this is generally true except for some special N values like $N = 2^k$). Thus, the solution of (27) is secured at all orders, since no 'kernel' monomials satisfying $\mathbf{m} = \mathbf{n}$ appear in (26). Despite its formal consistency, it is well known that the procedure outlined above yields a **divergent** series due to the accumulation of **small divisors**. Here we shall explore the non-resonant behavior of the full spectrum. The **diophantine character** of the linear frequencies Ω_i can be demonstrated numerically. A diophantine condition means that the small divisors satisfy an inequality of the form

$$|\mathbf{l} \cdot \mathbf{\Omega}| \geq \frac{\gamma}{|\mathbf{l}|^\tau} \text{ for all } \mathbf{l} \in \mathbb{Z}^N, |\mathbf{l}| \neq 0 \tag{28}$$

with $\gamma = const$, $\tau = O(N)$.

For each curve defined by:

$$a_{min}(r) = \min\{|\mathbf{l}\cdot\mathbf{\Omega}|, \text{for all } \mathbf{l}\in\mathbb{Z}^N \ |\mathbf{l}| = r\} \tag{29}$$

the ordinate gives the absolutely minimum divisor $a_{min}(r)$ as a function of r which, by the method of construction of formal integrals, coincides with the order at which this minimum divisor appears in the series for the first time. We find that the minimal divisors exhibit a power-law behavior $a_{min}(r) \sim r^{-\tau}$, where τ for each curve is determined by numerical experiments.

Within the limits of the small maximum value of N for which the calculation can be explicitly carried out, we find that the diophantine exponents τ show a clear tendency to increase linearly with N, by a relation of the form $\tau \sim 0.7N$ within the range of available data. Thus, in all heuristic considerations below we set $\tau \sim N$.

Nekhoroshev stability of FPU-trajectories with exponential localization

Estimates of the long-term stability of the FPU trajectories now follow directly from the asymptotic properties of the series (24).

To obtain them, it suffices to demonstrate that, for a suitable choice of r, the truncated series

$$\Phi_{j,r} = \Phi_j^{(2)} + \Phi_j^{(4)} + \ldots + \Phi_j^{(r)} \tag{30}$$

represents an **approximate** integral of motion, for times exponentially long in the inverse of a small parameter. In our case, it is possible to demonstrate the approximate constancy of (30) for FPU-trajectories exhibiting exponential localization, at the optimal order $r = r_{opt} \sim 1/\varepsilon$, where the variations of $\Phi_{j,r}$ become exponentially small in the inverse of the specific energy ε.

More precisely, the time derivative of the quantity (30) is given by

$$\frac{d\Phi_{j,r}}{dt} = R_{j,r} \equiv \left\{ \Phi_j^{(r)}, H_4 \right\} \ . \tag{31}$$

The quantity $R_{j,r}$ is called the **remainder function** of $\Phi_{j,r}$ at the normalization order r. Consider the family of FPU-trajectories started in the vicinity of the q-breather solutions with q_0 varying as $q_0 = 1, 2, \ldots$ in systems with $N = 2q_0\mu$ particles respectively, where μ is a constant satisfying $\mu \in \mathbb{N}, \mu >> 1$. These q_0 -breathers represent physically equivalent solutions in systems of progressively higher N.

The exact q_0 -breathers are periodic with a frequency Ω_{q_0}, which, in view of the adopted dependence of q_0 on N, are independent of N. On the other hand, an FPU-trajectory started in the vicinity of a q_0-breather need not be periodic, but we may assume that only the modes $j = (2k+1)q_0$, $k = 0, 1, 2, \ldots$ effectively participate in it. It can be shown that the size of the remainder function for such FPU-trajectories, as a function of r, can be estimated by

$$||R_r|| \sim \mathcal{B}_*((r-2)!)^{\frac{\mu+1}{2}} \varepsilon^{(\mu+1)r/2} \ , \tag{32}$$

where the constant $\mathcal{B}_*$ depends only on β. Eq.(32) yields essentially the magnitude of time variations of the approximate integrals truncated at order r.

One clearly sees the asymptotic character of the formal integral series from this equation. In particular, despite the heuristic character of estimate (32), we clearly recognize that such an estimate results from the partial control of the accumulation of small divisors **due to the particular profile of the energy localization** (19), which crucially affects the estimate (32). Of course, the compensation of small divisors thus produced is not complete and therefore the series is asymptotic. Nevertheless, the dependence of all estimates on N is removed.

The optimal order of truncation is found by taking the logarithm of (32) and using Stirling's formula $\log n! \approx n \log n - n$, as well as $r - 2 \approx r$ for r large. We thus find:

$$\log(||R_r||) \sim \log \mathcal{B}_* + \frac{\mu+1}{2} \left[r \left(\log r - 1 \right) + r \log \varepsilon \right]$$

The optimal normalization order is estimated as the value of r where $d \log ||R_r|| / dr \sim 0$, i.e.

$$r_{opt} \sim \frac{1}{\varepsilon} \ . \tag{33}$$

The optimal value of the remainder is then

$$||R_{opt}|| \sim \exp \left(-\frac{\mu+1}{2\varepsilon} \right) \tag{34}$$

i.e. the time variations of the integrals $\Phi_{j,opt}$ are exponentially small in $1/\varepsilon$. Finally, the choice $q_0 = \mu/2N$ was selected so that the underlying q-breathers have the same localization profile as the q-tori with constant fraction $M = s/N$. Thus, the generalization of the result to FPU-trajectories started close to the q-tori is straightforward.

Conclusions

1) We introduced the concept of q-tori in FPU lattices, which represent a generalization of the concept of q-breathers. The q-tori have low dimensionality $s << N$, and arise from the continuation of motions with s independent frequencies of the unperturbed problem.

2) We presented analytical and numerical evidence demonstrating that the complete explanation of the paradox of the FPU recurrences is based not only on the q-breathers analysis of Flach at al. (2005), but also on the existence and localization of **q-tori of low dimensionality**, forming exponentially stable “natural packets".

3) We obtained an estimate for the average harmonic energies $E^{(k)}$ of the modes excited at the kth order of the perturbation theory, in terms of the total energy E

$$E^{(k)} \sim \frac{E}{s}\left(\frac{C^2\beta^2(N+1)^2E^2}{\pi^4 s^4}\right)^k \quad . \tag{35}$$

which is similar with the estimate for q-breathers (Flach et al. 2006), with s replaced by q_0.

4) We showed that **exponential localization of the energy** occurs also in the case of the q–tori describing the “natural packets" discussed by other authors and thus completed the explanation of the FPU paradox inspired by the concept of q–breathers.

5) We calculated FPU solutions lying on q-tori by employing the method of Poincaré-Lindstedt series. Based on estimates of the leading terms of these series, we provided a theoretical law yielding the average exponential localization of the energy in Fourier space for solutions on q-tori. The most important outcome of this analysis is that, if the fraction s/N is kept constant, the localization profile depends on the **specific energy** $\varepsilon = E/N$ of the system, and thus it turns out to be independent of N.

6) We explored numerically the relevance of q-tori of dimension s to FPU-trajectories close to them, started by exciting s modes only. The localization laws found theoretically for q-tori describe well the localization of energy in Fourier space for the FPU-trajectories as well. We then gave numerical evidence of the existence of a critical energy above which the slope of the localization profile tends to stabilize and equipartition is expected to occur.

7) We examined the stability of q-tori using a numerical criterion provided by the GALI indices and provided numerical evidence demonstrating that the localization in Fourier space persists for values of the energy well above the value at which the underlying q-tori turn from stable to unstable.

8) Finally, we obtained a result on the Nekhoroshev stability of FPU trajectories having initially an exponentially localized profile, similar to their neighboring q-breathers or q-tori. In particular, we demonstrated how this particular choice of profile can be exploited to remove the bad dependence of the estimates of Nekhoroshev stability on N. This implies that the stability time should be exponentially long in $1/\varepsilon$, and substantiates the importance of the metastability scenario in interpreting the famous paradox of the FPU recurrences.

References

1. H. Christodoulidi, C. Efthymiopoulos and T. Bountis [2009], ”Energy localization on q–tori, Nekhoroshev stability and the interpretation of FPU recurrences”, PRE, to appear.
2. Skokos, Ch., Bountis, T. and Antonopoulos, Ch. [2007], “Geometrical properties of local dynamics in Hamiltonian systems: the Generalized Alignment Index (GALI) method”, Physica D **231**, 30.
3. T. Bountis, "Stability of Motion: From Lyapunov to N - Degree of Freedom Hamiltonian Systems", [2006], "Nonlinear Phenomena and Complex Systems", vol. **9**(3) ,209 -239, 2006.
4. Antonopoulos, Ch., Bountis, T. C. and Skokos, Ch., [2006], “Chaotic Dynamics of N–Degree–of–Freedom Hamiltonian Systems”, International Journal of Bifurcation and Chaos, vol.**16**(6), 1777-1793 , June 2006.
5. Antonopoulos, Ch. and Bountis, T., [2006], “Stability of Simple Periodic Orbits and Chaos in an FPU Lattice”, PRE**73**, 056206, 1-8 (2006).
6. Skokos, Ch., Antonopoulos, Ch., Bountis, T. C. and Vrahatis, M. N. [2004], “Detecting Order and Chaos in Hamiltonian Systems by the SALI Method", *J. Phys. A*, **37**, pp. 6269 – 6284.